Cranial biomechanics, bite force, and function of the endocranial sinuses in *Diprotodon optatum*, the largest known marsupial

Alana C. Sharp[1, 2] & Thomas H. Rich[3]

[1] School of Science and Technology, University of New England, Armidale, New South Wales, Australia

[2] School of Earth, Atmosphere and Environment, Monash University, Clayton, Victoria, Australia

[3] Sciences Department, Museum Victoria, Melbourne, Australia

Short title: Cranial biomechanics of *Diprotodon*

Corresponding author:

Dr Alana C. Sharp

School of Science and Technology

University of New England

Armidale, NSW, Australia, 2351

E-mail: asharp6@une.edu.au

Phone: +61 2 6773 2128

Mobile: +61 4 0142 6384

Abstract

The giant extinct marsupial *Diprotodon optatum* has unusual skull morphology for an animal of its size, consisting of very thin bone and large cranial sinuses that occupy most of the internal cranial space. The function of these sinuses is unknown as there are no living marsupial analogues. The finite element method was applied to identify areas of high and low stress and estimate the bite force of *Diprotodon* to develop hypotheses on the function of the extensive cranial sinuses. Detailed three-dimensional models of the cranium, mandible and jaw adductor muscles were produced. In addition, manipulations to the *Diprotodon* cranial model were performed to investigate changes in skull and sinus structure including a model with no sinuses (sinuses 'filled' with bone) and a model with a midsagittal crest. Results indicate that the cranial sinuses in *Diprotodon* significantly lighten the skull while still providing structural support, a high bite force and low stress, indicating the cranium may have been able to withstand higher loads than those generated during feeding. Data from this study supports the hypothesis that pneumatisation is driven by biomechanical loads and occurs in areas of low stress. The presence of sinuses is likely to be a by-product of the separation of the outer surface of the skull from the braincase due to the demands of soft tissue including the brain and the large jaw adductor musculature, especially the temporalis. In very large species, such as *Diprotodon*, this separation is more pronounced, resulting in extensive cranial sinuses due to a relatively small brain compared to the size of the skull.

Key Words: Finite element analysis; Marsupialia; morphology; bite force; Sinus; pneumatisation

Introduction

The extinct *Diprotodon optatum* is the largest marsupial that ever lived, weighing an estimated 2 to 3 metric tons as adults (Wroe et al., 2004). Like many other Australian megafauna species, *Diprotodon* became extinct during the late Pleistocene, about 45,000 years ago. As a generalist browser-grazer, *Diprotodon* would have thrived feeding on grasses, herbs and small shrubs, and was well adapted to exploit different habitats (Webb, 2009; Gröcke, 1997).

Despite its large size, the cranium of *Diprotodon* is remarkably lightweight, and is composed of thin cranial bone pneumatized by extensive cranial sinuses. Cranial sinuses are air-filled, mucosal lined chambers resulting from bone remodelling in areas where biomechanical demands are low and structurally unnecessary bone is resorbed. The size and complexity of cranial sinuses in vertebrates varies with different groups (Badlangana et al., 2011; Farke, 2010; Siliceo et al., 2011; Curtis et al., 2015; Sharp, in press). In very large mammals like *Diprotodon*, the braincase is often separated from the outside surface of the skull by frontal sinuses, epitympanic sinuses, squamosal sinuses and parietal sinuses. In most cases, large sinuses are crisscrossed by many thin-walled trabeculae, which form a convoluted network of air cavities (Badlangana et al., 2011; Farke, 2010; Sharp, in press). It is unclear whether these struts provide support as the outer bone that forms the dorsal surface of the skull separates from the braincase, or if they are simply a by-product of rapid pneumatisation (Farke, 2008; Tanner et al., 2008; Zollikofer & Weissmann, 2008)

In *Diprotodon*, the cranial sinuses including the frontal, parietal and squamosal sinuses have expanded to surround the middle ear cavity and braincase in all but the ventral surface (Sharp, 2014). Large sinuses have also been recorded in other large extinct diprotodontian marsupials (Murray, 1992; Black et al., 2010; Sharp, in press). In juveniles,

the outer surface of the skull and the inner surface of the braincase are separated by a thick layer of cancellous bone called the diploe. During ontogeny, the two surfaces separate and air cavities form as the diploe expands, increasing the size of the cavities as the separation continues. In a recent study comparing the variation in volume of the cranial sinuses and brain cavity in extinct and extant vombatiform marsupials, Sharp (in press) concluded that the cranial sinuses expand to accommodate the temporalis muscle because the relatively small brain in these species does not allow sufficient surface area for their attachment. It was identified that as skull size gets larger, the sinuses display positive allometric growth, and the brain negative allometric growth, so that in very large animals the sinuses are relatively larger and the brain is relatively smaller than in smaller animals. The cranial sinuses in smaller extant species including koalas (*Phascolarctos cinereus*) and wombats (*Vombatus* and *Lasiorhinus*) are restricted to the frontal bone and do not expand into the parietals. Conversely, in all extinct species analysed, varying in size from *Propalorchestes* (approximately 40 kg; Sharp, in press) to *Diprotodon optatum* (approximately 2-3 tons; Wroe et al. (2004)), the cranial sinuses expand into the parietal and occipital bones. This supports the hypothesis of Moss & Young (1960) who suggested that the demands of soft tissue, including the area for attachment of the masticatory musculature and the size of the brain, may be the main driver of sinus expansion.

Many functional hypotheses have been put forward to explain the presence of cranial sinuses (Keir, 2009; Márquez, 2008; Witmer, 1997; Farke, 2010; Moss & Young, 1960). However, it is likely there is no single function in all taxa. As previously noted, the most likely explanation is that sinuses form where bone is not structurally necessary, resulting in a lighter skull than if the same space was filled with cancellous bone. However, derived functions for pneumatised regions have also been hypothesized in special cases including assisting in thermoregulation of the brain in the giraffe (Mitchell & Skinner, 2003, 2004;

Ganey et al., 1990; Dyce et al., 2002), providing shock absorption during head-butting or neck-sparring (Badlangana et al., 2011; Davis et al., 1996; Schaffer & Reed, 1972), serving as a resonance chamber for the production of low frequency sounds in giraffe and cassowary (von Muggenthaler et al., 1999; Leakey & Walker, 1997; Naish & Perron, 2014) and dissipation of stress over the skull during mastication in bone-cracking hyenas, extinct borophagine canids and bamboo-eating pandas (Tanner et al., 2008; Buckland-Wright, 1978, 1971; Joeckel, 1998).

In the case of *Diprotodon*, the convex frontoparietal region of the cranium and the associated large sinuses may be a more optimal way to increase the attachment area of the temporalis muscle than would a plate-like sagittal crest for an animals of such size with a proportionally small braincase (Sharp, 2014; Sharp, in press). A plate-like sagittal crest is a common feature among mammals for attachment of the temporalis muscle. Sagittal crests are common in felids, canids, primates and some marsupial taxa, including the extant koala; however, sagittal crests are not present in any large extinct marsupial megafauna and the reason is unknown. Compared to a solid plate-like sagittal crest, expended sinuses may provide a broader area for attachment of the temporalis muscle while keeping the skull lightweight.

The invasion of large sinuses from the frontal into the parietal bones in some hyaenids and borophagine canids (an extinct subfamily of bone-crushing dogs) may function to dissipate stress away from the facial region during bone-cracking (Tanner et al., 2008; Werdelin, 1989; Joeckel, 1998; Tseng, 2009). The presence of sinuses increases structural support and resists bending stresses imposed by the temporalis muscle when compared to a solid, plate-like sagittal crest. This function appears to be enhanced when the frontal bone is domed, as in *Diprotodon*. The braincase in *Diprotodon* is too small to allow for sufficient attachment of the temporalis muscle, so expansion of the sinuses may be in response to the

119 growth of these muscles during development, and the presence of sinuses may result in a
120 more mechanically efficient skull. Alternatively, the shape and size of sinuses may reflect the
121 loads placed on the skull, including loads imposed during mastication.

122 The extraordinary preservation of near-complete skulls of *Diprotodon* found at
123 Bacchus Marsh in Victoria, Australia, has provided an opportunity to investigate their
124 morphology and function. In the present study, finite element (FE) analysis was applied to
125 explore the function of the extensive cranial sinuses in *Diprotodon*. The FE method is a
126 computational tool used to predict the distribution of stress and strain for complex structures
127 in response to applied loads, taking into account the elasticity and geometry of the structure
128 (Richmond et al., 2005; Rayfield, 2007; Bright, 2014). To apply the method to a complex
129 structure like a skull, the structure is simplified into a finite number of elements of simple
130 geometry, typically triangles or squares for 2D models and cubes or tetrahedra for 3D
131 models. An advantage of the FE method is that it is non-invasive and can be applied to fossil
132 taxa. Furthermore, the geometry of digital models can be manipulated to test functional
133 implications of different morphology.

134 Three main hypotheses for the function of the sinuses in *Diprotodon* were tested
135 during loads generated by the masticatory muscles. The first is that the sinuses serve to
136 lighten the skull; second, that they primarily function to dissipate stress; and finally that they
137 are a by-product of rapid pneumatisation to provide a greater surface area for the attachment
138 of the temporalis muscle. Three different FE models were constructed to explore the
139 mechanical and functional effect of morphological change: (1) a skull model with normal
140 sinus morphology maintained; (2) a hypothetical model with the cranial sinuses completely
141 filled with bone (‘filled-sinus’ model) to test if this region experiences low stress and strain
142 and if sinuses form where bone is not structurally necessary; and (3) a model with the sinuses
143 removed and a solid plate-like sagittal crest added (‘crest’ model) to test if a pneumatised

domed frontalparietal region is more mechanically efficient. If the 'filled-sinus' model experiences low or no stress over the frontoparietal region, but stress in other regions is similar to the normal model, this would indicate that sinuses develop where bone is not mechanically necessary, and that the external morphology of the skull is more important for skull function than the presence of sinuses. This would support both hypotheses that the sinuses lighten the skull while providing sufficient surface area for the attachment of the temporals muscle. If the distribution of stress is more even in the normal model compared to both the filled and sagittal crest model, this would suggest that the presence of sinuses allows the skull to dissipate stress more evenly then when the space is filled with bone. If a stress dissipating effect is identified, this function may have evolved to accommodate high bite forces, which will also be estimated.

Material and methods

Data collection

A near complete cranium of *Diprotodon optatum* (NMV P31299), recovered from Pleistocene sediments at Bacchus Marsh in southern Victoria, Australia, was scanned by computed tomography (CT) using a Siemens Sensation 64 scanner (Siemens Medical Solutions) at St. Vincent's Public Hospital, Melbourne. Voxels were 0.586 x 0.586 mm and slice thickness and interslice distance was 0.6 mm and 0.3 mm, respectively, to produce 978 CT slices in the transverse plane. Two near-complete dentaries (NMV P151802 and NMV 157382), also recovered from Bacchus Marsh, were CT scanned using the same facilities and parameters to produce one composite lower jaw for reconstruction of the masticatory muscles. The dentaries were similar in size so minimal scaling or manipulation was necessary.

Model construction

The CT data were imported into the image processing software program Mimics 13.1 (Materialise), where manual editing of the CT slices took place to isolate the craniodental morphology from the inorganic matrix that remained inside some of the sinus cavities, and to generate STL surface files of the cranium and dentaries. The 3D surface files were then imported into Geomagic Studio (Geomagic, Inc.) to improve the quality of the surface mesh, and repair breaks and missing regions of the cranium, including the zygomatic arches. These missing regions were reconstructed using the mirroring tool of more complete areas, as well as reference from the morphology of the surrounding bone and other skull specimens with these regions preserved (notably NMV P150021). The model was then imported into Hypermesh (Altair Engineering Inc.), where a further series of steps were taken to ensure the quality of the surface mesh, including testing the aspect ratio of the triangles, the dihedral angle and the tetrahedral quality, before converting it to a solid 3D FE mesh composed of 4-noded tetrahedral elements (tet4; mean edge length of 1.805 mm) resulting in a model with 5,277,638 elements. The element size was chosen so that thin bones in the skull had two or more elements thickness to accurately predict the displacement of nodes within the model due to the applied loads. Quadratic 10-noded tetrahedral elements (tet10) could have achieved the same outcome due to the placement of an extra node along each element edge; however, the computational time was increased significantly using tet10 elements, and previous studies have demonstrated that models with a high number of tet4 elements produce more stable measurements compared to tet10 models (Bright & Rayfield, 2011; Tseng & Flynn, 2015b; Dumont et al., 2005). A lower jaw model was also constructed following the same method by combining the CT scans from two, near complete mandibles from the same

192 fossil site (NMV P151802 and NMV 157382). The mandible was used to align the muscle
193 force vectors but was excluded from the FE analysis.

194 In addition to the original model, two modified models were produced: a 'filled-sinus'
195 model and a 'crest' model (Figure 1). The original surface model was imported to Avizo
196 (Visage Imaging, Inc.) as a stereolithography (STL) file and converted to a series of 2D slices
197 using the 'ScanConvertSurface' module. The 'filled-sinus' model was constructed by
198 converting the sinus area from 'air' to 'bone', essentially filling in the space with elements
199 that were later assigned the material properties of bone, see below (Figure 2B). The 'crest'
200 model was produced by filling the sinuses and modifying the external geometry of the skull
201 by flattening the frontoparietal region and adding a midsagittal crest (Figure 2C). The
202 construction of this model was guided by observations of koala skulls, a smaller but related
203 species to *D. optatum* with a sagittal crest, and placental herbivores such as the Brazilian tapir
204 (*Tapirus terrestris*) that have a high, broad and solid sagittal crest. Based on these
205 observations, the height of the midsagittal crest was maintained at the same height as the
206 dorsal surface of the original skull and the frontoparietal region was flattened as much as
207 possible without modifying the location or shape of the orbits, braincase, or occipital crest.
208 Surface models were then produced and converted to 3D FE meshes composed of 4-noded
209 tetrahedral elements ('filled-sinus' model = 5,963,413 elements; 'crest' model = 4,998,012
210 elements). The average element size was kept the same between all models to eliminate
211 errors in model output and to allow differences between difference morphologies to be
212 evaluated.

213 Each FE mesh was then imported to Abaqus CAE v6.12 where material properties
214 and boundary conditions were applied. There are no data available summarising the material
215 properties of bone in marsupial skulls, and material properties are often altered during
216 diagenesis of fossils (Snively & Theodor, 2011; Tseng & Wang, 2010; Tseng, 2009; Oldfield

et al., 2012; Rayfield, 2007). Therefore, each model was assigned homogeneous and isotropic average values of Young's modulus (E = 20 GPa) and Poisson's ratio (ν = 0.3) for mammalian bone (Tseng et al., 2011; Erickson et al., 2002; Dumont et al., 2005; Tseng & Wang, 2010; Figueirido et al., 2014; Tseng & Flynn, 2015a). This may produce stiffer models with higher bite forces than models with multiple material properties incorporating cancellous bone in areas where the skull is thick. However, this methodology was considered suitable for the present study, which compares relative stress and strain values due to broad changes in morphology. It has also been shown that using multiple material properties has little effect on large-scale patterns of stress and strain compared to variation in model shape, so it was assumed that interpretations of the results from this study would not differ substantially from those if heterogeneous material properties were used (Strait et al., 2005; Walmsley et al., 2013).

Each model was constrained by a single node at both temporomandibular joints (TMJ) to simulate the jaw hinge during biting. The left TMJ was fully constrained against displacement in all axes, and the right TMJ was constrained to allow lateral displacement of the skull, so as not to over constrain the model. Over constraining the model may produce unrealistic stresses and strains due to the Poisson's effect (compression in one direction causing expansion in the other two directions) (Dumont et al., 2005). Relaxed constrained such as those used in this study have been shown to produce more accurate results than models constrained in all axes at both TMJs (Tseng & Flynn, 2015b). To simulate biting at various positions a single node was constrained at the bite points in the direction perpendicular to the occlusal plane. Biting scenarios were modelled to simulate bilateral biting at each molar and at the incisors with the muscles on both sides of the skull fully activated to estimate maximum possible bite force. The incisors in *Diprotodon* continuously grown throughout the animals' life so would require considerable use to keep them

functional. Therefore, biting at the incisors may have an important functional role that contributes to skull morphology. The molars, however, do not continuously grow and will primarily be used to mechanically process large quantities of vegetation before being swallowed.

Muscle forces were applied to the FE models by distributing the load for each muscle over the entire surface of its origin by estimating the attachment area from muscle scars present on the fossilized bone and through comparisons with extant marsupials. Muscle orientations were determined by creating a vector between the origin and the corresponding insertion on the mandible. The jaw adductor musculature was considered to involve three main components; the temporalis, masseter and pterygoid muscles. Each muscle group was modelled with two or three subdivisions based on published studies of marsupial jaw muscles (Turnbull, 1970; Tomo et al., 2007; Warburton, 2009; Crompton et al., 2008; Murray, 1998; Sharp & Trusler, 2015; Sharp, 2014). The muscles included are *masseter superficialis, masseter profundus, zygomaticomandibularis, temporalis superficialis, temporalis profundus, pterygoideus medialis* and *pterygoideus lateralis*. These muscles were digitally reconstructed in 3D in Avizo following a similar method used by Lautenschlager (2013) and Curtis et al. (2009) and described for *Diprotodon* in Sharp (2014). The muscle forces (Table 1) were estimated by measuring the cross-sectional area of the reconstructed muscles and multiplying by a constant value of intrinsic muscle stress, 0.3 N mm^{-2} (Weijs & Hillen, 1985; van Spronsen et al., 1989; Thomason, 1991; McHenry et al., 2007; Wroe et al., 2005; Cox et al., 2012; Strait et al., 2005; Rayfield, 2007).

Analysing Model Performance

The resultant force, or bite force, at each bite point was recorded from Abaqus for each of the models and the mechanical efficiency, or mechanical advantage, was compared by calculating the ratio of the bite reaction force to the applied muscle force (Dumont et al., 2009). This measure provides a scale independent estimate of the efficiency of the jaw lever system that is defined by the fulcrum (TMJ), the effort (muscle force) and the resistance (bite point) as a third-class lever.

Contour plots of von Mises (VM) stress, and maximum and median VM stresses, were extracted from Abaqus as an indicator of the strength of the structure. Structures with lower values of stress are less likely to fail under a given load and are considered stronger. In addition, models were also analysed by sampling stress values along the dorsal cranium. Seven landmarks were sampled along the midsagittal axis from the tip of the nasals to the occipital crest: 1) rostral-most contact between the nasal bones; 2) between the infraorbital foramina; 3) between the rostral-most point of the orbits; 4) between the post-orbital processes; 5) between the post-orbital constriction of the parietal bones; 6) half-way along the length of the braincase; and 7) at the caudal end of the sagittal crest. At each location, ten nodes were selected and the average VM stress was calculated. Total internal strain energy, a measure of energy efficiency or the stiffness of a structure, was also recorded for each model simulation. Structures with higher strain energy are more compliant and will deform more easily, store more energy and transmit less energy to the bite point (Dumont et al., 2009). Thus, stiffer models will be more efficient than compliant models.

Results

Bite force and mechanical efficiency

The bite force at the incisors, premolars and each molar along the tooth row was estimated and compared for each model (Table 2). The maximum bite force estimated for the original skull model of *Diprotodon* is 2374 N at the incisors and between 4118 and 11134 N at the cheek teeth from the premolar to the fourth molar. For all models, bite force and mechanical efficiency increased as the bite point moved from the incisors to the fourth molar. The normal model had slightly higher bite force at every bite location (approximately 10% and 5% higher than the 'filled-sinus' model and 'crest' model respectively), indicating that the internal structure of the sinuses may affect the biting performance of the skull. This difference may fall within the margin of error between the models; however, the error was minimised by keeping the element size the same between the models, and by applying homogenous material properties, limiting error that may be due to distribution of material properties within the models.

Stress distribution and strain energy

The area of highest stress for all models was the zygomatic arch. During incisor biting, the premaxilla also experienced high stress. The pattern of stress distribution in each model for incisor biting and first and fourth molar biting are displayed in figure 3. Despite the change in sinus structure between the models, the stress distribution stays relatively similar across the zygomatic arch, the palate, and the rostrum for all bite locations. The only major difference is stress over the frontal and parietal regions where the sinuses develop. Stress is more evenly spread across the dorsal surface of the normal skull. The 'crest' model shows a higher concentration of stress anterior to the frontoparietal region compared with the normal model, similar to observations in previous studies on other taxa (Tseng, 2009; Tanner et al., 2008). In the model with the sinuses filled with bone, almost zero stress is experienced over the

frontoparietal region. Stress within the skull is also low (Figure 4). In the normal model, low stress is experienced around the external bone of the frontoparietal sinuses and the structural struts within it, while in the 'filled-sinus' model, stress in this region is essentially zero. Stress distribution along the midsagittal plane is shown with landmarks from the tip of the nasals to the occipital crest in figure 5. Stress is highest in the normal model at all points along the midsagittal axis except point 2 where the 'crest' model is higher. The highest stress in the 'filled-sinus' and 'crest' models is located at point 2 in the nasal region. For the normal model, the highest stress is shifted posteriorly to point 4, located on the frontal. Also in figure 5 is a dorsal view with the skull roof cut-away showing the stress inside the sinuses. The 'filled-sinus' and 'crest' models have almost zero stress in this region.

Quantitative differences between the three models are displayed in figure 6 for biting at each molar and the incisors. The 'filled-sinus' model has the lowest median VM stress and strain at all bite points. Strain energy, an indicator of the stiffness of the model, is highest in the normal skull model, meaning it deforms more easily. This is expected, because thinner bone allows more deformation than thick solid bone.

Discussion

Bite force

The exceptionally high bite forces at the molar tooth row suggest that *Diprotodon* was able to consume a variety of food, including tough, fibrous grasses which require more work or energy to fracture the plant material (Sanson, 2006). Isotope analysis of fossil teeth revealed that *Diprotodon* consumed both C3 and C4 plants (Gröcke, 1997), allowing this species to thrive feeding on grasses, herbs and small shrubs, and exploit different habitats. However, the

low levels of stress across the cranium indicate that the skull could withstand greater forces than those generated by the jaw muscles during feeding. It has been suggested that high bite forces at the incisors allowed the largest fossil rodent *Josephoartigasia monesi* to use their incisors to dig for food or defend against predators (Cox et al., 2015). Since sexual dimorphism has been suggested as an explanation for a high degree of size variation in *Diprotodon* specimens, it is possible that *Diprotodon* used its massive incisors in male-male competition. This may be testable using FEA by applying large forces to the incisors to determine the loads that *Diprotodon* could withstand.

We cannot directly compare the bite force of *Diprotodon* to other large herbivores, such as elephants or rhinoceros, because bite force has not been recorded for these species, *in vivo* or *in vitro*. However, bite force has been estimated in some large herbivorous taxa including rodents and the giant panda (Cox et al., 2015; Christiansen & Wroe, 2007; Figueirido et al., 2014). The herbivorous giant panda (*Ailuropoda melanoleuca*) has an estimated maximum bite force of 1816 N at the carnassial (Christiansen & Wroe, 2007) and 1710 N at the second molar (Figueirido et al., 2014). In rodents, the largest fossil rodent (*Josephoartigasis monesi*, approximately 1000 kg) has an estimated bite force of 4165 N at the third molar (Cox et al., 2015). The bite forces estimated in *Diprotodon* are higher than those estimated in these species (4118 to 11134 N), possibly because *Diprotodon* is larger and has a relatively larger temporalis muscle. However, it must be noted that the methods used between these studies and the way the finite element models were constructed and loaded are different and, therefore, confidence in these comparisons is limited. It is also possible that this study overestimates the bite forces for *Diprotodon* due to the model being assigned homogenous material properties or modelled with single node constraints that could make the model stiffer than in real life. In addition, these bite forces are considered the

359 maximum possible bite forces and probably do not represent the bite forces during normal
360 mastication.

361

362 *Sinus function*

363 The normal model had the highest overall stress and strain of the three morphologies tested.
364 The thin bone that forms the external surface of the sinuses and the struts within, undergo
365 more deformation than the 'filled-sinus' and 'crest' models with solid bone in the frontal and
366 parietal regions. The 'filled-sinus' model had the lowest overall stress and strain, indicating it
367 is both strong and resistant to deformation. This is not unexpected since thick bone will not
368 deform as readily as thin bone. The pattern of stress distribution showed very little stress over
369 the frontal and parietal region where the sinuses develop. This is consistent with the
370 hypothesis that sinuses form where there is low, or no biomechanical stress. As described
371 previously, sinuses develop through a process called pneumatisation. Bone remodelling in
372 response to biomechanical demands results in the removal of structurally unnecessary bone,
373 and the deposition of bone to reinforce areas that experience higher levels of stress (Moss &
374 Young, 1960; Witmer, 1997; Farke, 2008, 2010). The frontoparietal region in *Diprotodon*
375 experiences very low stress and, therefore, thick bone in this area is unnecessary for structural
376 support.

377 The presence of sinuses may be a by-product of the separation of the outer surface of
378 the skull from the braincase, providing a larger area for the temporalis muscles that is not
379 offered by a the relatively small brain in *Diprotodon* (Sharp, in press). This was first outlined
380 by Moss & Young (1960) in their explanation of neurocranial growth, emphasising the
381 response of different functional components (an outer table, a diploe, and an inner table) to
382 the demands of soft tissue they support and protect. *Diprotodon* and many other marsupials

have proportionally larger temporalis muscles compared to placental herbivores such as ungulates (Turnbull, 1970; Sharp, 2014). The relative size of the jaw muscle complex is an important factor in cranial morphology, and assuming that very large marsupials like *Diprotodon* retained the jaw muscle proportions of ancestral marsupials, the bony architecture must also be retained despite a small braincase. Expansion of the sinuses provides the necessary surface area for the attachment of large temporalis muscles, while potentially increasing mechanical efficiency and lightening the skull.

The sinus volume of the *Diprotodon* specimen is 2675 cm^3, accounting for approximately 25% of the total cranial volume (Sharp, in press). Assuming bone density is approximately 1.5 g cm^{-3} (Hall, 2005), the 'filled-sinus' model would be 4.0 kg heavier than the real skull, or approximately 30% heavier when just considering the bone mass of the head. However, if the sinus region was filled with bone it would most likely be cancellous bone which is considerably less dense than compact bone. So, while the sinuses increase the amount of stress and deformation of the skull, this amount is very low and may be inconsequential compared to the benefit of a lighter skull.

There is some evidence to support the hypothesis that the cranial sinuses function to evenly dissipate stress from the bite point, posteriorly over the cranium away from the nasal region. In figure 5, the highest stress in the 'filled-sinus' and 'crest' models is located at the nasal bone (point 2), while in the normal model, the highest stress is shifted posteriorly to the frontoparietal region (point 4). In hyenas, the pattern of stress distribution follows an arch along the vaulted forehead, and the frontoparietal sinuses help to resist loads by dissipating stress over the skull surface (Tanner et al., 2008). This adaptation is thought to have evolved to provide a stronger structure for bone-cracking and prevent weak points occurring in the facial region that are prone to failure under very high bite forces. As an herbivore, bone-cracking is not required by *Diprotodon*, but as discussed earlier the bite force is still very

high, and the cranium may be able to withstand greater forces than those generated during feeding. Therefore, the skull appears to be "over-engineered" for biting at both the incisors and molars during loads generated by the masticatory muscles. Furthermore, as a very large mammal, *Diprotodon* would have consumed large quantities of food requiring long processing times and a high frequency of mastication cycles. The adaptation to dissipate stress more evenly over the skull could help to reduce the likelihood of fatigue failure caused by repetitive stress on the craniodental system, as has been suggested for the red panda (*Ailurus fulgens*) (Figueirido et al., 2014). The stress dissipating effect that the sinuses appear to provide may limit areas of high stress, decreasing the chances of failure over time.

The role of the trabeculae, or struts, within the sinuses was not tested in the present study. Previous research has demonstrated that the trabeculae may not have a function other than being a by-product of sinus formation (Farke, 2008). Some bovids have very few struts (e.g. *Alcelaphus* and *Damaliscus*), while others have elaborate strutting (e.g. *Ovis canadensis* and *Syncerus caffer*) (Farke, 2007; Farke, 2010). However, the morphology, or complexity of the struts was not correlated with behaviours such as head-butting. Instead, the complexity of sinuses was more strongly correlated with phylogeny. The configuration of trabeculae within the sinuses of *Diprotodon* is very simple; however, despite this simplicity they are unlikely to reduce the structural integrity of the skull, as indicated by the low stress observed in this study. The struts are more likely to correspond with cranial sutures. There is some evidence that the sinuses in other taxa do not cross sutural boundaries, and that the size and morphology of sinuses are restricted, or influenced, by sutures (Farke, 2007; Farke, 2010). In *Diprotodon*, the midsagittal strut, separating the frontal sinuses into left and right portions, corresponds to the interfrontal suture. A strut perpendicular to this, dividing the sinuses into anterior and posterior portions, is located at the frontoparietal suture. The frontal sinuses themselves have no further struts. The only other recorded species with such limited strutting

433 in the frontal sinus is the Hartebeest (*Alcelaphus buselaphus*) (Farke, 2007; 2010), so it is
434 unclear what determines the complexity of the trabecula network.

435 In future, biomechanical performance tests could also be applied to other extinct
436 marsupial megafauna, including *Zygomaturus*, and to extant megafauna such as elephants and
437 giraffes to examine the structure and function of sinuses in other species. Furthermore, the
438 mechanisms that might control the formation and morphology of the trabecula network
439 within the sinuses could be investigated through ontogenetic studies. It would be of
440 considerable interest to determine whether the strut patterns are based on phylogeny,
441 behavioural functions, biomechanical stress distribution, ontogenetic development, or
442 through a combination of these. Another possible step would be a comparative analysis of
443 large herbivores to investigate the hypothesis that herbivore skulls are overbuilt to reduce the
444 risk of fatigue failure.

445

446 **Conclusion**

447 This study is the first to examine the biomechanical performance of the skull and cranial
448 sinuses of an extinct herbivorous species of marsupial megafauna and illustrates that the
449 extensive cranial sinuses may benefit *Diprotodon* by providing adequate surface area for the
450 attachment of the temporalis muscle while also increasing mechanical efficiency of biting,
451 dissipating stress and lightening the skull. The presence of large sinuses is likely explained by
452 the pneumatisation of the frontal and parietal bones due to low mechanical stress and the
453 necessity for a large attachment area for the temporalis muscle that is not provided by the
454 relatively small surface area of the braincase. The sinuses in *Diprotodon* also significantly
455 lighten the skull while still providing structural support. The seemingly delicate-for-it's-size
456 cranium of *Diprotodon* is actually a remarkably strong structure that improves transmission

of muscle force into bite force. By comparing the original skull morphology with hypothetical morphologies including the construction of a midsagittal crest, this study shows that the combination of the externally domed frontals and an associated sinus allows for similar increases in surface area like a sagittal crest would, but is much better at dissipating stress, as has been shown in other taxa (Tanner et al., 2008; Tseng, 2009; Joeckel, 1998). The loads simulated in this study were those produced by the jaw muscles; the temporalis, masseter and pterygoids. The resultant bite force was high, but stress was still low over the cranium, which might indicate the cranium could withstand higher loads not generated during feeding. Higher forces may have been produced by using the incisors during competition with rival individuals or defense against predators. Alternatively, the low and evenly distributed stress over the cranium may reduce the likelihood of fatigue failure from prolonged and repetitive masticatory cycles. Finally, this study also demonstrates the utility of the FE method. The ability to experiment with altered morphologies in a non-invasive way provides opportunities to address questions of form-function relationships in extinct species where specimens are fragile or rare.

Acknowledgments

The authors would like to thank Museum Victoria for access to the specimens; Shelley O'Hara from St. Vincent's Hospital for CT scanning; Patricia Vickers-Rich and Tim Flannery for preparation of the specimens; Monash University for the doctoral scholarship awarded to A.C.S. and facilities and software used for this study; and, Elizabeth Dumont and Ian Grosse for assistance during the Finite Element Modeling in Biology workshop at the University of Massachusetts, Amherst. We would also like to thank the reviewers for their very helpful comments for improving this manuscript.

Author contributions

A.C.S. designed and carried out the study, analysed the results and contributed to the writing and editing of the manuscript. T.H.R. arranged access and CT scanning of the specimen and contributed to study design and editing of the manuscript.

References

Badlangana NL, Adams JW, Manger PR (2011) A comparative assessment of the size of the frontal air sinus in the giraffe (*Giraffa camelopardalis*). *The Anatomical Record: Advances in Integrative Anatomy and Evolutionary Biology,* **294,** 931-940.

Black KH, Archer M, Hand SJ, et al. (2010) First comprehensive analysis of the cranial ontogeny in a fossil marsupial - from a 15-million-year-old cave deposit in northern Australia. *Journal of Vertebrate Paleontology,* **30,** 993-1011.

Bright JA (2014) A review of paleontological finite element models and their validity. *Journal of Paleontology,* **88,** 760-769.

Bright JA, Rayfield EJ (2011) The response of cranial biomechanical finite element models to variations in mesh density. *The Anatomical Record,* **294,** 610-620.

Buckland-Wright JC (1971) The distribution of biting forces in the skulls of dogs and cats. *Journal of Dental Research,* **50,** 1168-1169.

Buckland-Wright JC (1978) Bone-structure and patterns of force transmission in cat skull (*Felis catus*). *Journal of Morphology,* **155,** 35-61.

Christiansen P, Wroe S (2007) Bite force and evolutionary adaptations to feeding ecology in carnivores. *Ecology,* **88,** 347-358.

Cox PG, Rayfield EJ, Fagan MJ, et al. (2012) Functional evolution of the feeding system in rodents. *Plos One,* **7,** e36299.

Cox PG, Rinderknecht A, Blanco RE (2015) Predicting bite force and cranial biomechanics in the largest fossil rodent using finite element analysis. *Journal of Anatomy*.

Crompton AW, Lieberman DE, Owerkowicz T, et al. (2008) Moter control of masticatory movements in the southern hairy-nosed wombat (*Lasiorhinus latifrons*). In *Primate craniofacial function and biology* (eds Vinyard CJ, Ravosa MJ, Wall CE). New York: Springer.

Curtis AA, Lai G, Wei F, et al. (2015) Repeated loss of frontal sinuses in arctoid carnivorans. *Journal of Morphology,* **276,** 22-32.

Curtis N, Jones MEH, Evans SE, et al. (2009) Visualising muscle anatomy using three-dimensional computer models - an example using the head and neck muscles of *Sphenodon*. *Palaeontologia Electronica,* **12,** 18-35.

Davis WE, Templer J, Parsons DS (1996) Anatomy of the paranasal sinuses. *Otolaryngologic Clinics of North America,* **29,** 57-74.

Dumont ER, Grosse IR, Slater GJ (2009) Requirements for comparing the performance of finite element models of biological structures. *Journal of Theoretical Biology,* **256,** 96-103.

Dumont ER, Piccirillo J, Grosse LR (2005) Finite-element analysis of biting behavior and bone stress in the facial skeletons of bats. *The Anatomical Record Part A-Discoveries in Molecular Cellular and Evolutionary Biology,* **283A,** 319-330.

Dyce KM, Sack WO, Wensing CJG (2002) *Textbook of Veterinary Anatomy,* W. B. Saunders Company, Philadelphia.

Erickson GM, Catanese J, Keaveny TM (2002) Evolution of the biomechanical material properties of the femur. *The Anatomical Record,* **268,** 115-124.

Farke AA (2007) Morphology, constraints, and scaling of frontal sinuses in the hartebeest, *Alcelaphus buselaphus* (Mammalia: Artiodactyla, Bovidae). *Journal of Morphology,* **268,** 243-253.

Farke AA (2008) Frontal sinuses and head-butting in goats: a finite element analysis. *Journal of Experimental Biology,* **211,** 3085-3094.

Farke AA (2010) Evolution and functional morphology of the frontal sinuses in Bovidae (Mammalia: Artiodactyla), and implications for the evolution of cranial pneumaticity. *Zoological Journal of the Linnean Society,* **159,** 988-1014.

Figueirido B, Tseng ZJ, Serrano-Alarcón FJ, et al. (2014) Three-dimensional computer simulations of feeding behaviour in red and giant pandas relate skull biomechanics with dietary niche partitioning. *Biology Letters,* **10,** 20140196.

Ganey T, Ogden J, Olsen J (1990) Development of the giraffe horn and its blood supply. *The Anatomical Record,* **227,** 497-507.

Gröcke DR (1997) Distribution of C3 and C4 plants in the late Pleistocene of South Australia recorded by isotope biogeochemistry of collagen in megafauna. *Australian Journal of Botany,* **45,** 607-617.

Hall BK (2005) *Bones and cartilage: developmental and evolutionary skeletal biology,* Academic Press.

Joeckel RM (1998) Unique frontal sinuses in fossil and living Hyaenidae (Mammalia, Carnivora): Description and interpretation. *Journal of Vertebrate Paleontology,* **18,** 627-639.

Keir J (2009) Why do we have paranasal sinuses? *The Journal of Laryngology & Otology,* **123,** 4-8.

Lautenschlager S (2013) Cranial myology and bite force performance of *Erlikosaurus andrewsi*: a novel approach for digital muscle reconstructions. *Journal of Anatomy,* **222,** 260-272.

Leakey M, Walker A (1997) *Afropithecus* function and phylogeny. In *Function, Phylogeny, and Fossils: Miocene Hominoid Evolution and Adaptations* (eds Begun DR, Ward CV, Rose MD), pp. 225-239. New York: Plenum Press.

Márquez S (2008) The Paranasal Sinuses: The Last Frontier in Craniofacial Biology. *The Anatomical Record: Advances in Integrative Anatomy and Evolutionary Biology,* **291,** 1350-1361.

McHenry CR, Wroe S, Clausen PD, et al. (2007) Supermodeled sabercat, predatory behavior in *Smilodon fatalis* revealed by high-resolution 3D computer simulation. *Proceedings of the National Academy of Sciences,* **104,** 16010-16015.

Mitchell G, Skinner JD (2003) On the origin, evolution and phylogeny of giraffes (*Giraffa camelopardalis*). *Transactions of the Royal Society of South Africa,* **58,** 51-73.

Mitchell G, Skinner JD (2004) Giraffe thermoregulation: a review. *Transactions of the Royal Society of South Africa,* **59,** 109-118.

Moss ML, Young RW (1960) A functional approach to craniology. *Anthropology,* **18,** 281-292.

Murray PF (1992) Thinheads, thickheads and airheads - functional craniology of some diprotodontan marsupials. *The Beagle: Records of the Museums and Art Galleries of the Northern Territory,* **9,** 71-87.

Murray PF (1998) Palaeontology and palaeobiology of wombats. In *Wombats* (eds Wells RT, Pridmore PA), pp. 1-9. Chipping Norton, Sydney: Survey Beatty.

Naish D, Perron R (2014) Structure and function of the cassowary's casque and its implications for cassowary history, biology and evolution. *Historical Biology*.

Oldfield CC, McHenry CR, Clausen PD, et al. (2012) Finite element analysis of ursid cranial mechanics and the prediction of feeding behaviour in the extinct giant *Agriotherium africanum*. *Journal of Zoology,* **286,** 163-170.

Rayfield EJ (2007) Finite element analysis and understanding the biomechanics and evolution of living and fossil organisms. *The Annual Review of Earth and Planetary Sciences,* **35,** 541-576.

Richmond BG, Wright BW, Grosse I, et al. (2005) Finite element analysis in functional morphology. *The Anatomical Record Part A-Discoveries in Molecular Cellular and Evolutionary Biology,* **283A,** 259-274.

Sanson GD (2006) The Biomechanics of Browsing and Grazing. *American Journal of Botany,* **93,** 1531-1545.

Schaffer WM, Reed CA (1972) The co-evolution of social behavior and cranial morphology in sheep and goats (Bovidae, Caprini). *Fieldiana Zoology,* **61,** 1-88.

Sharp AC (2014) Three dimensional digital reconstruction of the jaw adductor musculature of the extinct marsupial giant *Diprotodon optatum*. *PeerJ,* **2,** e514.

Sharp AC (in press) A quantitative comparative analysis of the size of the frontoparietal sinuses and brain in vombatiform marsupials. *Memoirs of Museum Victoria*.

Sharp AC, Trusler PW (2015) Morphology of the Jaw-Closing Musculature in the Common Wombat (*Vombatus ursinus*) Using Digital Dissection and Magnetic Resonance Imaging. *PLoS ONE,* **10,** e0117730.

Siliceo G, Salesa MJ, Antón M, et al. (2011) Comparative anatomy of the frontal sinuses in the primitive sabre-toothed felid *Promegantereon ogygia* (Felidae, Machairodontinae) and similarly sized extant felines. *Estudios Geológicos,* **67,** 277-290.

Snively E, Theodor JM (2011) Common functional correlates of head-strike behavior in the Pachycephalosaur *Stegoceras validum* (Ornithischia, Dinosauria) and combative Artiodactyls. *Plos One,* **6,** 1-26.

Strait DS, Wang Q, Dechow PC, et al. (2005) Modeling elastic properties in finite element analysis: how much precision is needed to produce an accurate model? *The Anatomical Record Part A,* **283A,** 275-287.

Tanner JB, Dumont ER, Sakai ST, et al. (2008) Of arcs and vaults: the biomechanics of bone-cracking in spotted hyenas (*Crocuta crocuta*). *Biological Journal of the Linnean Society,* **95,** 246-255.

Thomason JJ (1991) Cranial strength in relation to estimated biting forces in some mammals. *Canadian Journal of Zoology,* **69,** 2326-2333.

Tomo S, Tomo I, Townsend GC, et al. (2007) Masticatory muscles of the great-grey kangaroo (*Macropus giganteus*). *Anatomical Record,* **290,** 382-388.

Tseng ZJ (2009) Cranial function in a late Miocene *Dinocrocuta gigantea* (Mammalia: Carnivora) revealed by comparative finite element analysis. *Biological Journal of the Linnean Society,* **96,** 51-67.

Tseng ZJ, Flynn JJ (2015a) Are Cranial Biomechanical Simulation Data Linked to Known Diets in Extant Taxa? A Method for Applying Diet-Biomechanics Linkage Models to Infer Feeding Capability of Extinct Species. *PLoS ONE,* **10,** e0124020.

Tseng ZJ, Flynn JJ (2015b) Convergence analysis of a finite element skull model of *Herpestes javanicus* (Carnivora, Mammalia): Implications for robust comparative inferences of biomechanical function. *Journal of Theoretical Biology,* **365,** 112-148.

Tseng ZJ, McNitt-Gray JL, Flashner H, et al. (2011) Model sensitivity and use of the comparative finite element method in mammalian jaw mechanics: mandible performance in the gray wolf. *Plos One,* **6,** e19171.

Tseng ZJ, Wang X (2010) Cranial functional morphology of fossil dogs and adaptation for durophagy in *Borophagus* and *Epicyon* (Carnivora, Mammalia). *Journal of Morphology,* **271,** 1386-1398.

Turnbull WD (1970) Mammalian masticatory apparatus. *Fieldiana: Geology,* **18,** 149-356.

van Spronsen PH, Weijs WA, Valk J, et al. (1989) Comparison of jaw-muscle bite-force cross-sections obtained by means of magnetic resonance imaging and high resolution CT scanning. *Journal of Dental Research,* **68,** 1765-1770.

von Muggenthaler E, Baes C, Hill D, et al. (1999) Infrasound and low frequency vocalizations from the giraffe. Helmholtz resonance in biology. *Proceedings of Riverbanks Consortium. Presented at the regional Acoustical.Society of America Conference (2001) (http://www.animalvoice.com/giraffe.htm).*

Walmsley CW, Smits PD, Quayle MR, et al. (2013) Why the Long Face? The Mechanics of Mandibular Symphysis Proportions in Crocodiles. *PLOS ONE,* **8**.

Warburton NM (2009) Comparative jaw muscle anatomy in kangaroos, wallabies, and rat-kangaroos (Marsupialia: Macropodoidea). *The Anatomical Record,* **292,** 875-884.

Webb S (2009) Late Quaternary distribution and biogeography of the southern Lake Eyre basin (SLEB) megafauna, South Australia. *Boreas,* **38,** 25-38.

Weijs WA, Hillen B (1985) Cross-sectional areas and estimated intrinsic-strength of the human jaw muscles. *Acta Morphologica Neerlando-Scandinavica,* **23,** 267-274.

Werdelin L (1989) Constraint and adaptation in the bone-cracking canid *Osteoborus* (Mammalia: Canidae). *Paleobiology,* **15,** 387-401.

Witmer LM (1997) The evolution of the antorbital cavity of archosaurs: a study in soft-tissue reconstruction in the fossil record with an analysis of the function of pneumaticity. *Journal of Vertebrate Paleontology,* **17,** 1-76.

Wroe S, Crowther M, Dortch J, et al. (2004) The size of the largest marsupial and why it matters. *Proceedings of the Royal Society of London Series B-Biological Sciences,* **271,** S34-S36.

Wroe S, McHenry C, Thomason J (2005) Bite club: Comparative bite force in big biting mammals and the prediction of predatory behaviour in fossil taxa. *Proceedings of the Royal Society B-Biological Sciences,* **272,** 619-625.

Zollikofer CPE, Weissmann JD (2008) A Morphogenetic Model of Cranial Pneumatization Based on the Invasive Tissue Hypothesis. *The Anatomical Record: Advances in Integrative Anatomy and Evolutionary Biology,* **291,** 1446-1454.

660 **Tables**

661 **Table 1.** Muscle cross-sectional areas (CSA) and forces applied to each side of the skull for
662 each finite element model. The muscle forces were estimated based on the cross-sectional
663 area of reconstructed muscles is described in Sharp (2014).

Muscle	**CSA (cm^2)**	**Force (N)**
Deep temporalis	5096.39	1529
Superficial temporalis	1491.95	448
Temporalis Total	**6588.34**	**1977**
Zygomaticomandibularis	5182.75	1555
Deep masseter	1593.21	478
Superficial masseter	4887.63	1466
Masseter Total	**11663.59**	**3499**
Medial pterygoid	4438.50	1331
Lateral pterygoid	729.42	219
Pterygoid Total	**5167.92**	**1550**
Total	**23419.85**	**7026**

664

665

666 **Table 2.** Predicted bite force for each model for each biting location

Biting tooth	Bite force (N)		
	Normal	Filled-sinus	Crest
I	2374	2091	2245
PM	4118	3688	3939
M1	4493	4033	4333
M2	5418	4855	5154
M3	6886	6352	6747
M4	11134	10257	11129

667

668

669

Figures

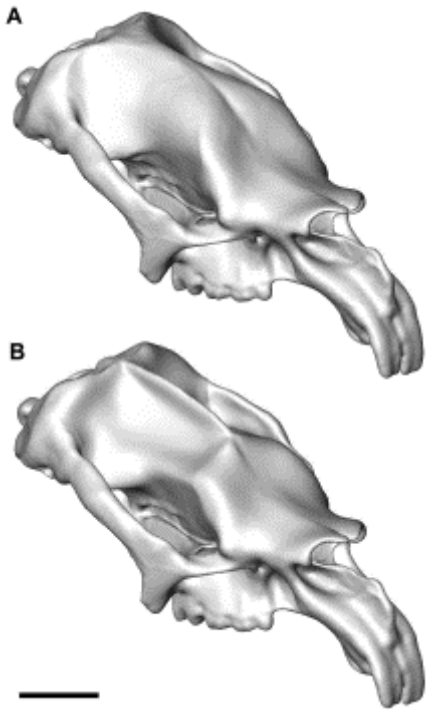

Figure 1. Skull surface models illustrating the different external morphologies of (A) the normal and 'filled-sinus' models and (B) the 'crest' model. Scale = 10 cm.

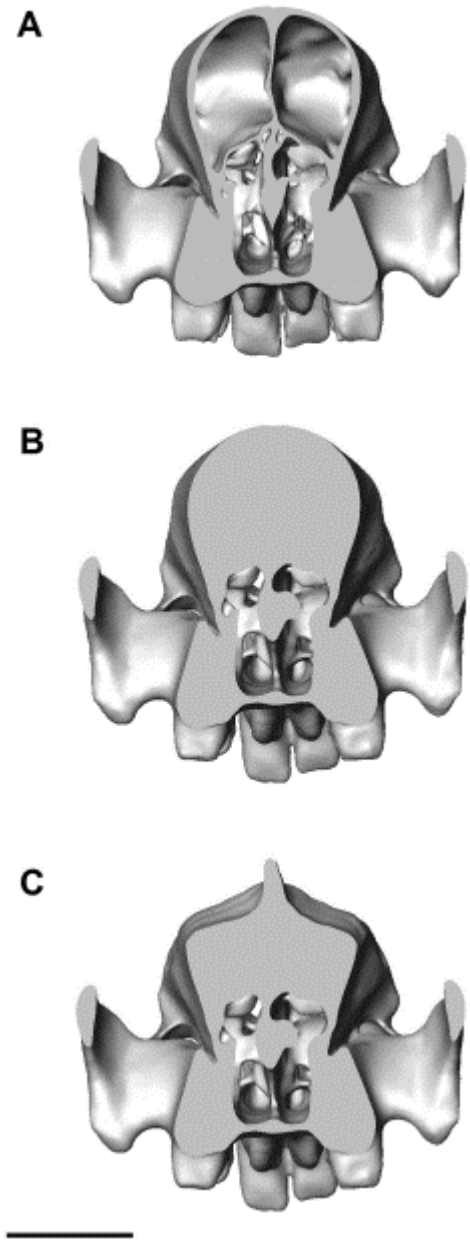

674

675 **Figure 2.** Frontal view cross-sections of the skull surface models illustrating the different
676 morphologies of (A) the normal model, (B) ‘filled-sinus’ model and (C) ‘crest’ model. Scale
677 = 10 cm.

678

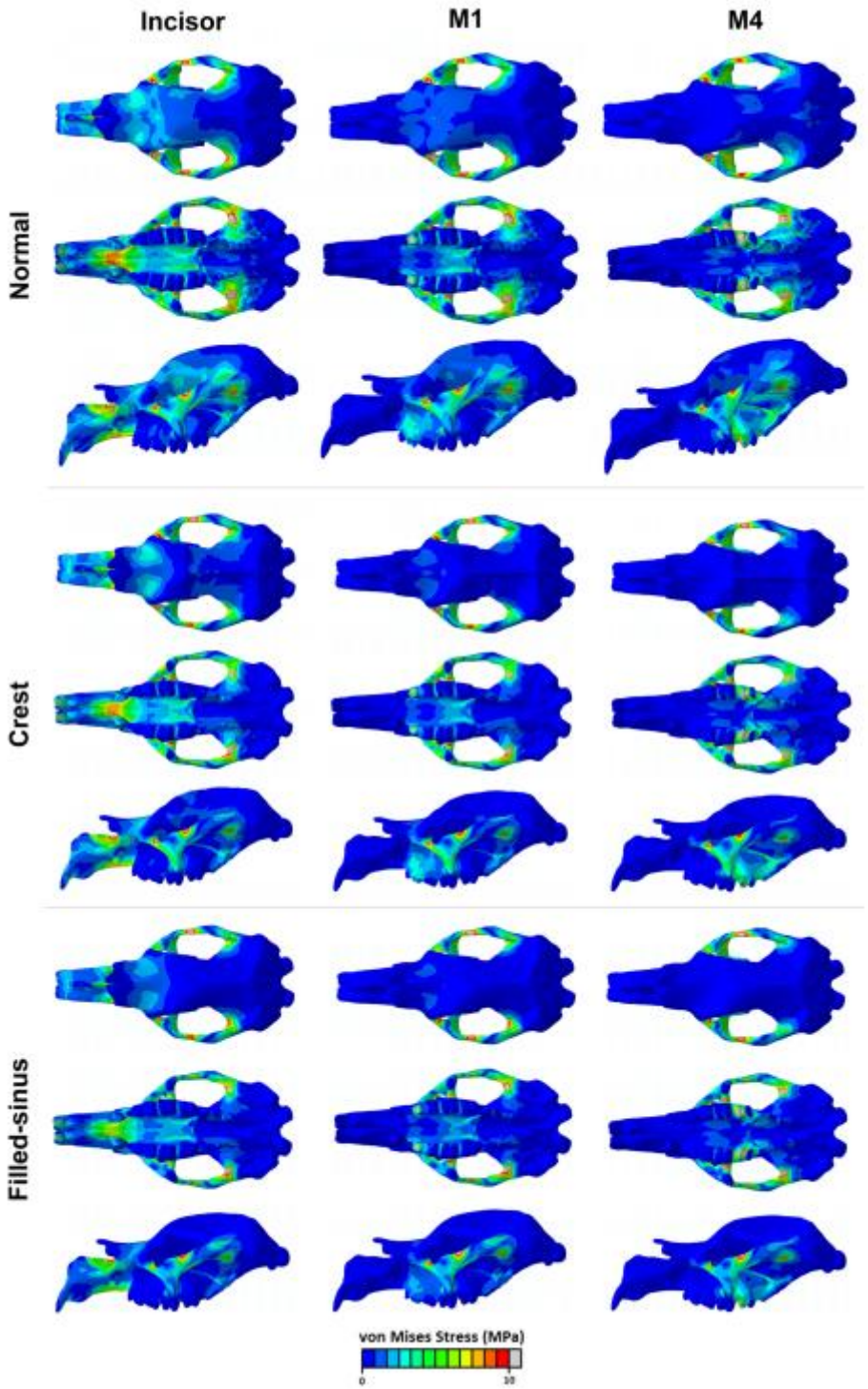

679

680 **Figure 3.** Von Mises stress patterns for the normal model, the 'crest' model and the 'filled-
681 sinus' model when bilateral biting at the incisors, first molar (M1) and fourth molar (M4).
682 Each model is shown in dorsal (top), ventral (middle) and lateral (bottom) views. Cool
683 colours represent areas of low VM stress, and warm colours high stress.

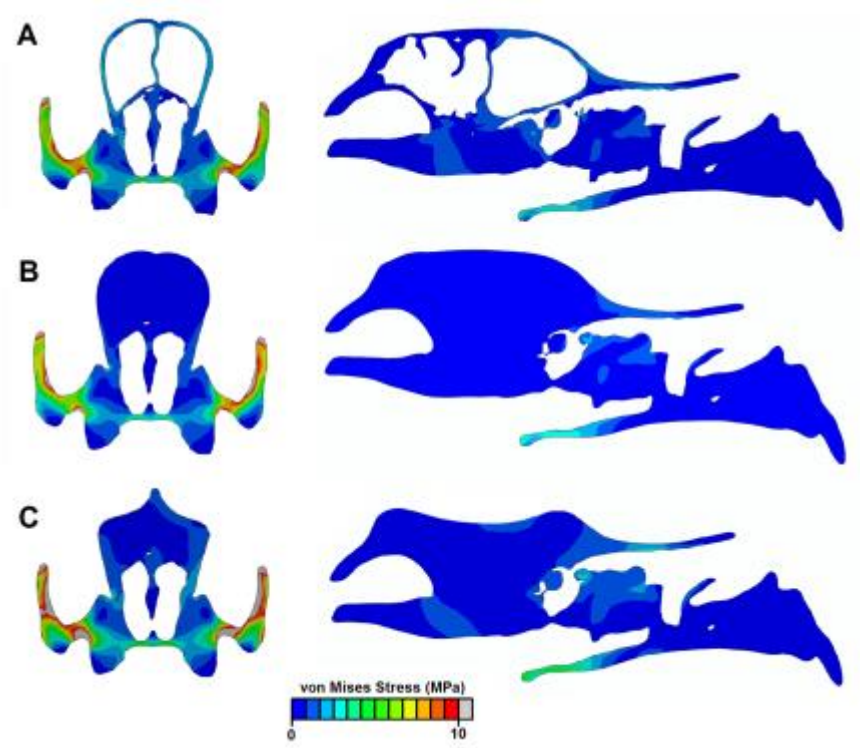

684

685 **Figure 4.** Von Mises stress patterns for the normal model (A), the 'filled-sinus' model (B)
686 and the 'crest' model (C) in transverse slices showing the frontal sinus (left) and sagittal
687 slices just offset from the midsagittal plane (right) when bilateral biting at the second molar.

688

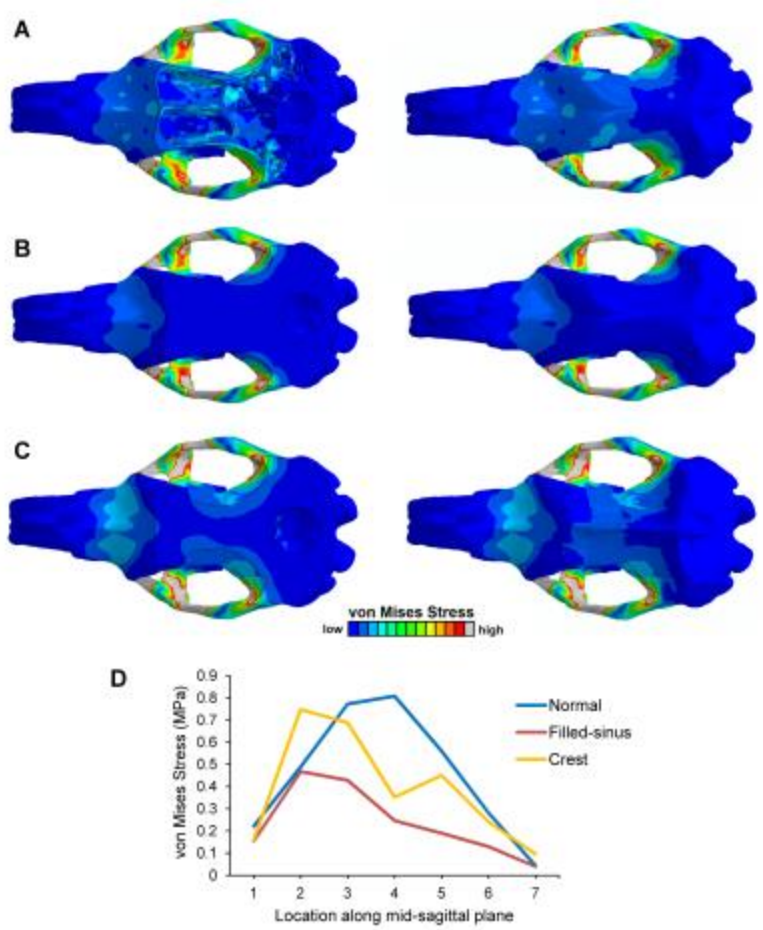

689

690 **Figure 5.** Von Mises stress patterns for the normal model (A), the 'filled-sinus' model (B)
691 and the 'crest' model (C) showing the dorsal surface (right) and with the dorsal skull roof cut
692 away to reveal the internal sinus morphology (left). The graph (D) displays von Mises stress
693 values at seven locations along the mid-sagittal axis for each of the models.

694

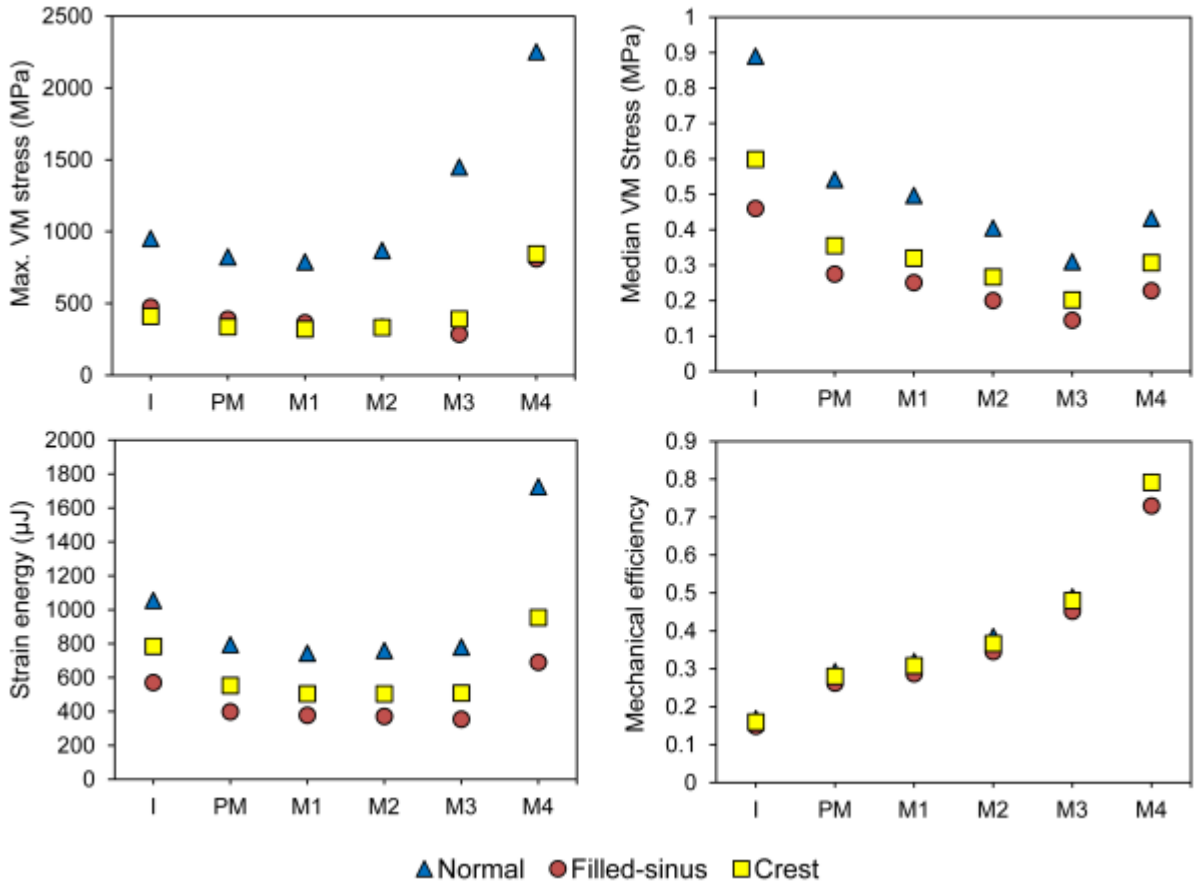

695

696 **Figure 6.** Biting performance during bilateral biting at each tooth in the normal cranial model
697 (blue triangle), 'filled-sinus' model (red circle) and 'crest' model (yellow square).
698 Abbreviations: I, incisor; PM, premolar; M1, first molar; M2, second molar; M3, third molar;
699 M4, fourth molar.

700